GRNND: A GPU-Parallel Relative NN-Descent Algorithm for Efficient Approximate Nearest Neighbor Graph Construction

Xiang Li
Nanjing University
Nanjing, China
652022230010@smail.nju.edu.cn

Qiong Chang*
Institute of Science Tokyo
Tokyo, Japan
q.chang@c.titech.ac.jp

Yun Li
Nanjing University
Nanjing, China
yli@nju.edu.cn

Jun Miyazaki
Institute of Science Tokyo
Tokyo, Japan
miyazaki@c.titech.ac.jp

Abstract

Relative Nearest Neighbor Descent (RNN-Descent) is a state-of-the-art algorithm for constructing sparse approximate nearest neighbor (ANN) graphs by combining the iterative refinement of NN-Descent with the edge-pruning rules of the Relative Neighborhood Graph (RNG). It has demonstrated strong effectiveness in large-scale search tasks such as information retrieval and related tasks. However, as the amount and dimensionality of data increase, the complexity of graph construction in RNN-Descent rises sharply, making this stage increasingly time-consuming and even prohibitive for subsequent query processing. In this paper, we propose GRNND, the first GPU-parallel algorithm of RNN-Descent designed to fully exploit GPU architecture. GRNND introduces a disordered neighbor propagation strategy to mitigate synchronized update traps, enhancing structural diversity, and avoiding premature convergence during parallel execution. It also leverages warp-level cooperative operations and a double-buffered neighbor pool with fixed capacity for efficient memory access, eliminate contention, and enable highly parallelized neighbor updates. Extensive experiments demonstrate that GRNND consistently outperforms existing CPU- and GPU-based methods. GRNND achieves 2.4 to 51.7× speedup over existing GPU methods, and 17.8 to 49.8× speedup over CPU methods.

Keywords

RNN-Descent, Parallel Approximate Nearest Neighbor Search, Graph Construction, GPU Acceleration

1 Introduction

Approximate Nearest Neighbor Search (ANNS) is a fundamental technique for large-scale high-dimensional data analysis, with widespread applications in information retrieval[10, 12, 16, 17, 31], natural language processing[29, 34, 36], and computer vision[1, 2, 11]. By tolerating a small accuracy loss, ANNS provides significant gains in scalability and search efficiency. In particular, graph-based ANNS methods stand out for their excellent trade-off between accuracy and speed, relying on a pre-constructed proximity graph for efficient querying. NN-Descent [5] represents a foundational method for constructing approximate k-NN graphs via iterative refinement. Based on it, two main strategies have emerged. The first builds a dense k-NN graph and applies pruning to obtain a sparser structure, such as NSG [7], SSG [6], and CAGRA [27]. The second integrates pruning directly into the construction process to obtain sparse graphs from the outset, as in NSW [23] and its GPU variant GANNS [37], HNSW [24] and RNN-Descent [26], thereby reducing the additional computation overhead introduced by dense pre-construction and subsequent pruning.

Within the direct-construction family, NSW offers simplicity and good navigability, but relies on randomized insertions that can produce uneven degrees and quality variance at scale. HNSW improves accuracy and robustness through hierarchical layering and heuristic pruning, but its incremental, order-dependent insertions and dynamic memory use introduce strong sequential dependencies and irregular memory behavior, which hinder parallelization. RNN-Descent, recently proposed by Ono et al. [26], is the current state-of-the-art for direct graph construction. Integrates the iterative propagation strategy of NN-Descent with edge pruning based on the Relative Neighborhood Graph (RNG) criterion [13]. This combination enables the construction of high-quality sparse graphs and consistently outperforms previous methods across multiple benchmarks.

With increasing amount and dimensionality of data, the cost of ANN graph construction grows rapidly, largely attributed to high-dimensional distance evaluations and neighbor maintenance tasks such as candidate sorting, deduplication, and redirection. Consequently, construction time often becomes the dominant stage in the end-to-end ANN retrieval pipeline, delaying or even preventing subsequent query processing [21, 22, 28]. In this context, Graphics Processing Units (GPUs) offer massive parallelism and memory bandwidth [8, 14, 20], and have shown great promise in accelerating

the online search stage of ANNS [30, 35, 38]. However, translating construction to GPUs has yielded limited gains without carefully structured algorithms [3, 4, 18, 19], and as a result, efficient graph construction on GPUs remains challenging [25, 33]. In particular, the original design of RNN-Descent assumes sequential iteration, ascending-order neighbor updates, and fine-grained dynamic memory access, which conflict with the GPU execution model. Direct parallelization leads to premature convergence: vertices update neighbors in the same ascending order without feedback, causing unnecessary reinsertion, dense local connections, and suppressed exploration. These issues prevent effective pruning and trap the graph in low-quality states.

To overcome these limitations, we propose GRNND, the first GPU-parallel algorithm of RNN-Descent. GRNND retains the core iterative refinement principles of RNN-Descent, but systematically redesigns its execution strategy and memory organization to align with the GPU architecture. It targets three key challenges: (1) avoiding premature convergence, (2) replacing dynamic memory with a fixed-capacity double-buffered neighbor pool, and (3) reducing control divergence and memory contention. The contributions of this paper can be summarized as follows:

- **Disordered neighbor propagation**: Instead of updating in ascending order, GRNND evaluates the candidate neighbors in randomized order, which avoids premature convergence, reduces unnecessary reinsertion, and promotes structural diversity.
- **Warp-level cooperative operation**: Each vertex is updated by a single warp using warp-level primitives (e.g., ballot, shuffle), enabling efficient distance computation and insertion with minimal control divergence and no global synchronization.
- **Fixed-capacity double-buffered pool**: Dynamic allocations are replaced by two fixed-size buffers per vertex, ensuring lock-free updates, efficient memory access, and natural alignment with warp-level operations.
- **Reverse edge sampling**: Rather than inserting reverse edges exhaustively, GRNND samples a subset each iteration, reducing computation while maintaining graph quality and exploration.

On RTX 4090, GRNND delivers 2.6 to 48.3× speedup over GPU baselines and 27.1 to 49.8× over CPU baselines. On RTX 6000 Ada, the corresponding ranges are 2.4 to 51.7× (GPU) and 17.8 to 26.2× (CPU), confirming consistent advantages across hardware platforms.

The remainder of this paper is organized as follows. Section 2 presents background information. Section 3 describes our GPU-parallel algorithm. Section 4 reports the experimental evaluation. Section 5 reviews related work and Section 6 concludes the paper.

2 BACKGROUND

For clarity, the notations used throughout this paper are summarized in Table 1.

2.1 Approximate Nearest Neighbor Search

The Approximate Nearest Neighbor Search (ANNS) aims to retrieve vectors close to a query $\mathbf{q} \in \mathbb{R}^d$ by trading exactness for

Table 1: Notation used throughout the paper.

Symbol	Meaning
V	Vertex set (dataset)
E	Edge set
$v \in V$	A vertex
n	A neighbor of v
N_v	Candidate neighbor set of v
N_v'	Refined neighbor set of v
$d(v_1, v_2)$	Distance function between vectors v_1 and v_2
S	Number of initial neighbors per vertex
R	Pool capacity (maximum neighbors per vertex)
T_1	Number of outer iterations
T_2	Number of inner iterations
ρ	Reverse-edge sampling ratio

improved efficiency. A typical ANNS system consists of two stages: index construction and online querying. Graph-based methods have emerged as one of the most effective approaches due to their superior trade-off between accuracy and efficiency [34]. They are based on a navigable proximity graph, where the quality of the graph largely determines search performance. Sparse graphs with adaptive neighbor sets often support more efficient navigation than uniform k-NN graphs, but their construction is computationally costly. During querying, performance is usually evaluated using two metrics: Recall@k and Queries Per Second (QPS). Recall measures accuracy as the fraction of true nearest neighbors retrieved, while QPS quantifies the number of queries processed per unit of time, indicating the efficiency of the search process.

2.2 RNN-Descent Algorithm

Algorithm 1 RNN-Descent Algorithm

1: **Input:** V, N_v, S, R, T_1, T_2
2: **Output:** Graph(V, E)
3: $\forall v \in V$: INITIALIZATION(v, S, N_v)
4: **for** $t_1 = 1$ to T_1 **do**
5:     **for** $t_2 = 1$ to T_2 **do**
6:         $\forall v \in V$: UPDATE_NEIGHBORS(v, R, N_v)
7:     **end for**
8:     **if** $t_1 \neq T_1$ **then**
9:         $\forall v \in V$: ADD_REVERSE_EDGES(v, R, N_v)
10:     **end if**
11: **end for**

RNN-Descent begins with a randomly initialized S-NN index and iteratively refines the graph by applying the RNG criterion. For a vertex v with two candidate neighbors n_1, n_2, both neighbors are retained only if:

$$d(n_1, v) < d(n_1, n_2) \wedge d(n_2, v) < d(n_1, n_2). \tag{1}$$

In other words, if n_1 and n_2 are closer to each other than either is to v, then the edge between them takes precedence over their connections to v. As shown in Figure 1, the vertex v is initially connected to two neighbors n_1 and n_2. Since n_2 is closer to n_1 than

to v, the edge between v and n_2 is removed and replaced by an edge between n_1 and n_2. The complete algorithm is presented in
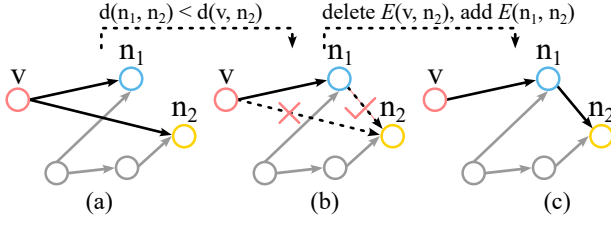

Figure 1: Neighbor refinement of vertex v under the RNG criterion. (a) Initial candidate neighbors; (b) RNG-based edge pruning; (c) Refined neighbor set of v.

Algorithm 1 and consists of three key steps: (1) random initialization of neighbor pools (line 3), (2) iterative refinement based on the RNG criterion (line 6), and (3) insertion of reverse edges to maintain structural diversity and avoid premature convergence (line 9).

Each vertex sequentially refines its candidate list N_v, as detailed in Algorithm 2. First, N_v is sorted by ascending distance $d(v, n)$ and duplicates are removed (line 3). The first neighbor (i.e., closest) is always accepted and added to N_v'. Each subsequent candidate $n \in N_v$ (line 5) is compared with all previously accepted neighbors $n' \in N_v'$ (line 7). If any n satisfies $d(n, n') \leq d(v, n)$ (line 8), n is excluded from N_v' and redirected to $N_{n'}$ (lines 9–11). Otherwise, n is retained and added to N_v' (line 15).

Algorithm 2 UPDATE_NEIGHBORS

1: **Input:** $v \in V$, candidate neighbors N_v
2: **Output:** Refined neighbors N_v'
3: Sort N_v by ascending $d(v, n)$ and remove duplicates
4: Retain top R closest candidates in N_v
5: **for** $n \in N_v$ **do**
6:   $valid \leftarrow$ true
7:   **for** $n' \in N_v'$ **do**
8:     **if** $d(n, n') \leq d(v, n)$ **then**
9:       $valid \leftarrow$ false
10:       $N_{n'} \leftarrow N_{n'} \cup \{n\}$
11:       **break**
12:     **end if**
13:   **end for**
14:   **if** $valid$ **then**
15:     $N_v' \leftarrow N_v' \cup \{n\}$
16:   **end if**
17: **end for**

Over iterations, the graph may prematurely converge to suboptimal configurations due to the strict RNG constraint. To prevent this, RNN-Descent inserts reverse edges at the end of each outer iteration (except the last). These additional connections, which may violate the RNG criterion, introduce structural diversity and promote continued refinement in the next iteration.

3 Parallel RNN-Descent on GPU

This section first analyzes the challenges of parallelizing RNN-Descent on GPUs and then presents our proposed GRNND.

3.1 Challenges in Parallelizing RNN-Descent

Although RNN-Descent is highly effective on CPUs, its neighbor update mechanism is inherently sequential, and thus unsuitable for direct GPU parallelization. Figure 2a illustrates this sequential process: Each vertex sorts and deduplicates its candidate neighbors, then iteratively applies the RNG criterion in ascending order. Take vertex 1 as an example. Its closest neighbor, vertex 2, is always retained. The remaining candidates, such as vertices 4 and 5, are evaluated against this retained set. For example, vertex 4 is closer to vertex 2 than to vertex 1, so it is excluded from the pool of vertex 1 and redirected to vertex 2. This step-by-step process enables progressive refinement. Each vertex updates after others and can incorporate their structural improvements. Crucially, each candidate is compared to the closest neighbor retained in the central vertex. This relative evaluation ensures that redirection decisions are optimal locally and topologically coherent.

Algorithm 3 GRNND Algorithm

1: **Input:** $V, N_v, S, R, T_1, T_2, \rho$
2: **Output:** $Graph(V, E)$
3: **for all** $v \in V$ **in parallel do**
4:   INITIAL_NEIGHBORS(v, S, N_v)
5: **end for**
6: **for** $t_1 = 1, 2, \ldots, T_1$ **do**
7:   **for** $t_2 = 1, 2, \ldots, T_2$ **do**
8:     **for all** $v \in V$ **in parallel do**
9:       UPDATE_NEIGHBORS_PARALLEL(v, N_v)
10:     **end for**
11:   **end for**
12:   **if** $t_1 \neq T_1$ **then**
13:     **for all** $v \in V$ **in parallel do**
14:       REVERSE_EDGE_SAMPLING(v, N_v, ρ)
15:     **end for**
16:   **end if**
17: **end for**

This relative comparison, enabled by sequential updates, is central to RNN-Descent's ability to refine the graph progressively on CPUs. However, when all vertices update their neighbors in parallel on GPUs, this sequential refinement is lost. In direct parallel implementation (Figure 2b), vertices follow the same ascending-order rule and update independently without awareness of structural changes elsewhere in the graph. Such uniform update behavior leads to premature convergence, a failure mode characterized by three compounding effects. First, many vertices redirect neighbors to the same central vertex, producing overly dense local structures that reduce graph diversity and navigability. Second, unnecessary reinsertion occurs when neighbors discarded by one vertex are concurrently reintroduced by others, essentially undoing pruning decisions. Third, exploration suppression emerges when uniform update behavior prevents the graph from discovering structurally diverse regions. Together, these effects degrade the constructed graph, undermining RNG pruning and ultimately reducing search accuracy. In addition, direct GPU implementations also suffer from irregular memory access and frequent dynamic allocations when maintaining per-vertex neighbor pools, further limiting scalability.

(a) Serial iteration: neighbor updates occur sequentially, enabling stepwise propagation of structural information.

(b) Parallel sorted iteration: each vertex independently updates in ascending order, breaking propagation chains and leading to local convergence traps.

(c) Parallel disordered iteration: candidate updates follow no fixed order, restoring stochastic propagation and enabling exploration beyond local optima.
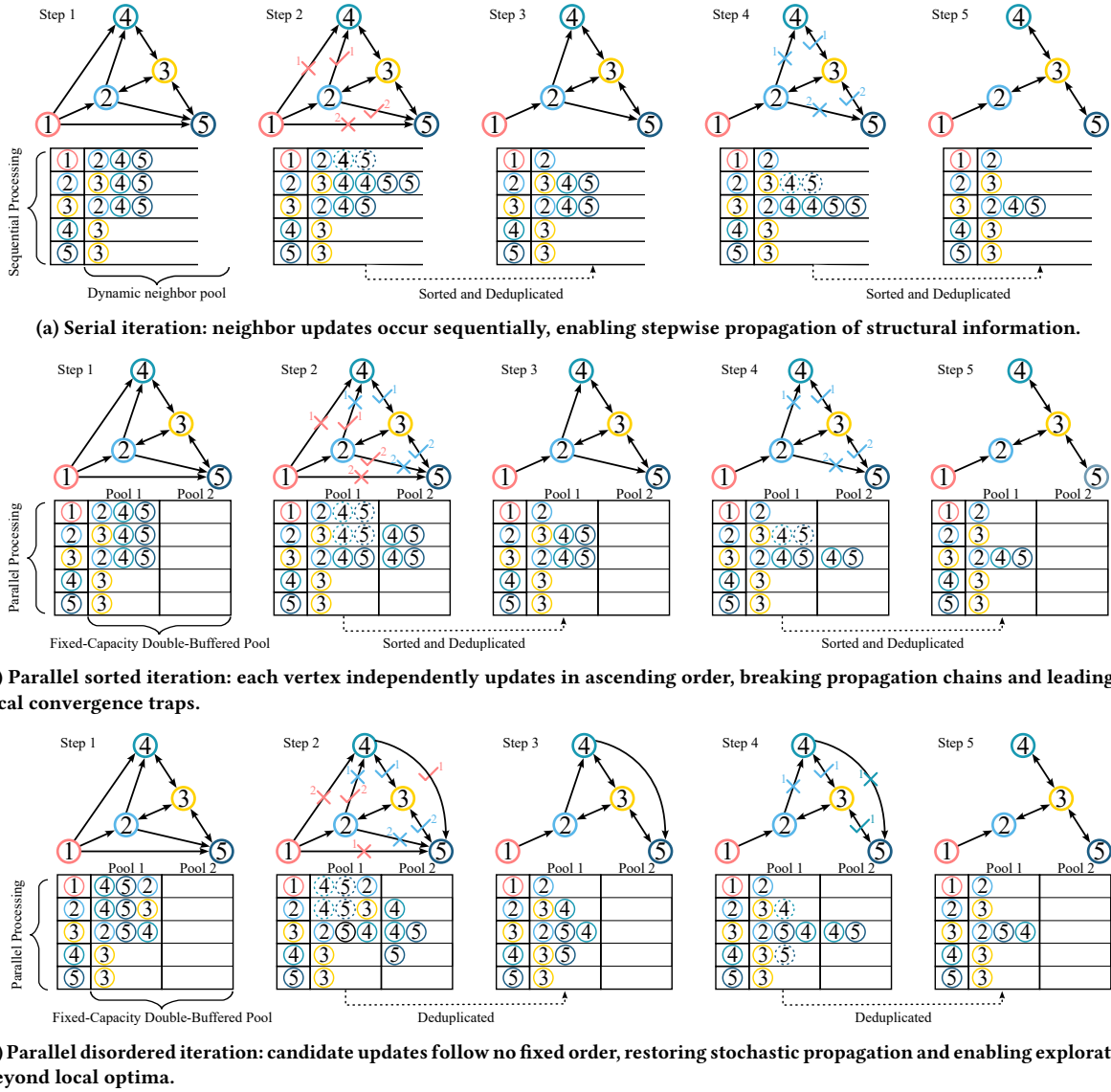
Figure 2: Comparison of serial vs. parallel execution in RNN-Descent. While serial scheduling enables gradual global optimization, direct parallelism with sorted updates breaks propagation order and leads to premature local convergence. Disordered parallel updates restore exploration capability by injecting randomness into the update paths.

3.2 Overall GRNND Framework

To overcome the limitations of parallel RNN-Descent, we propose **GRNND**, a GPU-native redesign of the algorithm. GRNND preserves the iterative refinement principle of RNN-Descent but systematically restructures its update mechanism, memory model, and control flow to exploit massive parallelism. GRNND is composed of four key components: (1) disordered neighbor propagation to break premature convergence; (2) warp-level cooperative operations for fine-grained parallelism; (3) fixed-capacity double-buffered pools to avoid dynamic memory allocation; and (4) reverse edge sampling to maintain connectivity without excessive overhead. These components are integrated into a unified parallel pipeline.

As shown in Algorithm 3, all vertices initialize in parallel with S random neighbors (lines 3–5). The algorithm runs T_1 outer iterations, each consisting of T_2 warp-level update rounds. In every round, all vertices apply disordered propagation (lines 8–10), which samples candidate pairs at random and applies RNG-based redirection. After each outer iteration (except the last), reverse edges are inserted for a sampled subset (ratio ρ) to maintain connectivity and diversity (lines 13–15). Throughout, warp-level primitives and fixed-size double buffers ensure efficient computation, safe concurrent updates, and regular memory access.

3.3 Disordered Neighbor Propagation

To avoid premature convergence caused by parallel ascending-order updates, we introduce a disordered neighbor propagation strategy tailored for GPU execution. Unlike the CPU implementation, which processes candidates in strictly ascending distance order, our approach evaluates them in randomized order. This breaks fixed update patterns and reduces symmetry across concurrent updates. For each vertex v, random neighbor pairs (n_i, n_j) are sampled from its candidate pool and the RNG criterion is applied:

$$n_{\text{close}} = \arg\min_{x \in \{n_i, n_j\}} d(v, x), \; n_{\text{far}} = \arg\max_{x \in \{n_i, n_j\}} d(v, x),$$

$$\text{if } d(n_i, n_j) < \max(d(v, n_i), d(v, n_j)) \Rightarrow n_{\text{far}} \mapsto N_{n_{\text{close}}}, \quad (2)$$

where v, n, d, and N denote the vertex, neighbor, distance, and candidate list, respectively.

Algorithm 4 UPDATE_NEIGHBORS_PARALLEL

1: **Input:** V, R, $pool_1[v]$, $pool_2[v]$ //double-buffered N_v
2: **for all** $v \in V$ **in parallel do**
3:     **for** random neighbor pairs $(n_i, n_j) \in pool_1[v]$ **do**
4:         $d_{ij} \leftarrow$ WARP_DISTANCE(n_i, n_j)
5:         **if** $d_{ij} < \max(d(v, n_i), d(v, n_j))$ **then**
6:             $n_{\text{close}} \leftarrow$ closer(n_i, n_j), $n_{\text{far}} \leftarrow$ farther(n_i, n_j)
7:             WARP_INSERT$(n_{\text{far}}, n_{\text{close}}, pool_2[n_{\text{close}}])$
8:             mark $n_{\text{far}} \leftarrow \bot$
9:         **end if**
10:     **end for**
11:     **for all** $n \in pool_1[v]$ **do**
12:         **if** $n \neq \bot$ **then**
13:             WARP_INSERT$(n, v, pool_2[v])$
14:         **end if**
15:     **end for**
16: **end for**
17: **Clear** $pool_1[\;]$ // reset N_v for next round
18: **Swap** $pool_1[\;] \leftrightarrow pool_2[\;]$ // swap pointers

---

This disordered strategy preserves the logic of the RNG criterion while introducing controlled randomness to break the synchronization that hinders convergence. As illustrated in Figure 2c, the vertices can evaluate distant candidates (e.g., 4 and 5) before their closest neighbor (e.g., vertex 2). In such cases, redirection may occur toward previously unseen nodes, encouraging exploration of structurally diverse regions. Since each vertex executes randomized updates independently, global update trajectories naturally diverge. This mitigates synchronization, reduces unnecessary reinsertion, and improves pruning effectiveness. Over time, the graph converges more stably and exhibits greater structural diversity.

Algorithm 4 summarizes the parallel execution. In each round (line 3), the vertices simultaneously sample candidate pairs (line 4), calculate distances using warp-level primitives (line 5), and apply the RNG condition. If satisfied, the farther neighbor is redirected to the closer one (lines 6-10).

Although randomization may cause some close neighbors to be retained in later rounds rather than immediately, repeated iterations and fixed double-buffered pools ensure their eventual preservation, yielding a stable balance between exploration and refinement and enabling reliable convergence with greater structural diversity.

3.4 Warp-Level Cooperative Operations

GRNND adopts a warp-level cooperative execution model to perform all stages of neighbor updates, including distance computation, deduplication, and insertion, as shown in lines 5, 8, and 14 of Algorithm 4. Instead of assigning one thread per vertex or per neighbor, this often leads to control flow divergence and irregular memory access. GRNND delegates the full update process of each vertex to a single warp. This design is better aligned with the GPU hardware model and ensures efficient execution.

Algorithm 5 WARP_DISTANCE(n_i, n_j)

1: **Input:** vectors x_i, x_j of dimension D
2: **Output:** Euclidean distance $d(x_i, x_j)$
3: $tid \leftarrow$ thread_id_in_warp(), $sum \leftarrow 0$
4: **for** $d = tid; d < D; d+ = 32$ **do**
5:     $sum \leftarrow sum + (x_i[d] - x_j[d])^2$
6: **end for**
7: **for** $offset = 16; offset \geq 1; offset = offset/2$ **do**
8:     $sum \leftarrow sum + \_shfl\_down(sum, offset)$
9: **end for**
10: **return** $\sqrt{sum}$ // Only lane 0 holds final result

---

A critical performance stage is high-dimensional distance computation. As illustrated in Algorithm 5, GRNND assigns a single warp to compute the distance between two vectors. Each vector is divided into segments, and all warp threads collaborate to process one segment in parallel (lines 3-6). Within each segment, every thread loads a single dimension from both vectors, computes the squared difference, and accumulates the result locally (line 5). Once all segments are processed, a warp-wide reduction aggregates the partial results to produce the final distance (line 8). As illustrated in Figure 3, the computation has three stages: Step 1, all warp threads collaboratively load and process the first segment in parallel; Steps 2 to $n-1$, the warp sequentially iterates over the remaining segments in the same manner; Last step, a warp-wide reduction aggregates the partial sums into the final distance.

Warp-level cooperation also extends to neighbor insertion. To prevent redundant entries in the candidate list, GRNND uses warp-level ballot operations to perform set membership checks. As shown in Figure 4, each warp loads a segment of the pool into registers and compares the candidate neighbor against existing entries. The primitive ballot returns a bitmask indicating which threads detected a match. If no match is found, the warp continues scanning the next segment; otherwise, insertion is skipped. This strategy enables fast, register-level filtering without requiring global synchronization. When a new neighbor is accepted, the warp either inserts it into an available slot or replaces an existing neighbor if the pool is full. In the replacement case, the warp uses max-reduction and ballot operations to locate the farthest neighbor, which is replaced only if the new candidate is closer. All insertions are performed using atomic operations to ensure correctness under concurrent access.

As detailed in Algorithm 6, GRNND implements warp-level insertion through a structured three-stage process. Lines 2 to 8 perform warp-level deduplication using ballot primitives; if the candidate neighbor already exists, the insertion is skipped. Lines 10 to 14 handle direct insertion when the pool is not yet full. If the pool is
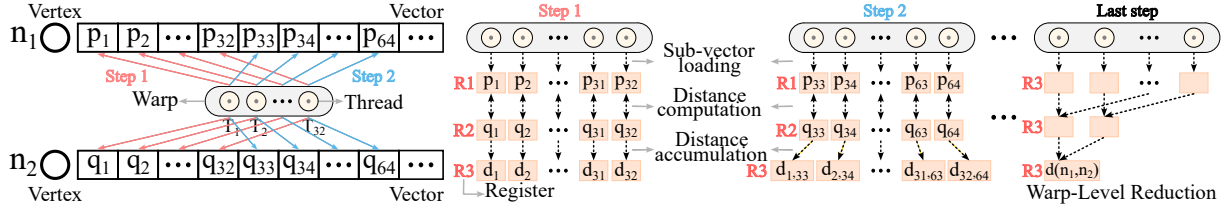
Figure 3: Warp-level distance computation: a single warp loads sub-vectors from two aligned inputs, computes squared differences in parallel, and performs warp-wide reduction.
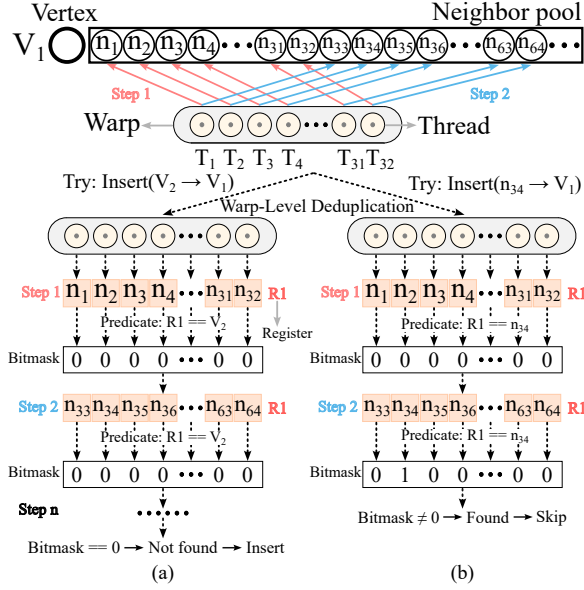

Figure 4: Efficient warp-level deduplication for candidate insertion using ballot function. (a) Insertion Allowed: V_2 not found in V_1's candidate set; (b) Insertion Skipped: n_{34} already exists in V_1's candidate set.

full, lines 16 to 26 perform a warp-level max-reduction to locate the farthest neighbor and replace it only if the new candidate is closer.

By encapsulating neighbor updates within warp-local routines, GRNND achieves: (1) uniform control flow with minimal divergence, (2) fully coalesced and efficient memory access, and (3) safe updates without inter-warp synchronization. This design transforms the inherently sequential update logic of RNN-Descent into a scalable, deterministic, and parallel-safe routine.

3.5 Fixed-Capacity Double-Buffered Pool

In CPU-based RNN-Descent, each vertex maintains a dynamic neighbor pool that is iteratively sorted, deduplicated, and truncated to keep the top-R neighbors. This relies on sequential updates and safe, fine-grained memory access. On GPUs, however, concurrent vertex updates cause race conditions and synchronization overhead, while per-vertex dynamic arrays in global memory incur heavy costs from frequent allocations and atomic operations. To address these issues, GRNND adopts a fixed-capacity double-buffered pool design. Each vertex is assigned two static buffers of size R: one

---

Algorithm 6 WARP_INSERT($n_{far}, pool_{close}$)

1:   $tid \leftarrow$ thread_id_in_warp(), $mask \leftarrow 0$
2:   // Step 1: Warp-level deduplication
3:   **for** $i = tid; i < R; i+ = 32$ **do**
4:     $mask \leftarrow mask \mid \_ballot(pool_{close}[i] == n_{far})$
5:   **end for**
6:   **if** $mask \neq 0$ **then**
7:     **return**   // Already exists, skip insertion
8:   **end if**
9:   // Step 2: Direct insertion if pool not full
10: $count \leftarrow$ number of valid entries in $pool_{close}$
11: **if** $count < R$ **then**
12:     $pool_{close}[count] \leftarrow n_{far}$
13:     **return**
14: **end if**
15: // Step 3: Pool full, replace farthest neighbor if closer
16: $max\_dist \leftarrow -\infty, rep\_idx \leftarrow -1$
17: **for** $i = tid; i < R; i+ = 32$ **do**
18:     $d \leftarrow d(n_{close}, pool_{close}[i])$
19:     **if** $d > max\_dist$ **then**
20:       $max\_dist \leftarrow d, rep\_idx \leftarrow i$
21:     **end if**
22: **end for**
23: $max\_dist \leftarrow$ warp_max(max_dist)
24: **if** $d(n_{close}, n_{far}) < max\_dist$ **and** $tid == rep\_idx$ **then**
25:     $pool_{close}[tid] \leftarrow n_{far}$
26: **end if**

---

for reading and one for writing. During iteration t, the read buffer holds the current neighbor set, while the write buffer accumulates filtered updates.

Figure 2 illustrates the update procedure: for each neighbor pair (n_i, n_j) in the read buffer (pool 1), the RNG condition is applied. If the condition is not satisfied, the farther neighbor is redirected and inserted into the write buffer (pool 2) of the closer vertex. After all pairwise evaluations, the surviving neighbors from pool 1 are also copied into pool 2, subject to the same filtering rules. Once the update completes, the pointers of the two buffers are swapped: pool 2 becomes the new pool 1 for the next iteration. This behavior is captured in lines 12 to 19 of Algorithm 4, where the retained neighbors are reinserted and the buffers are cleared and swapped. This double-buffered design eliminates dynamic memory allocation and fine-grained synchronization, while enabling deterministic, conflict-free, in-place neighbor updates under parallel execution. By

preserving iteration-level consistency, it stabilizes convergence and becomes a key building block of GRNND's GPU pipeline, supporting scalable and lock-free neighbor updates under massive parallelism.

3.6 Reverse Edge Sampling

Following disordered neighbor propagation, the graph already exhibits high structural diversity and exploratory connectivity. In this setting, inserting reverse edges for all neighbors incurs unnecessary overhead with diminishing returns. To balance graph quality and efficiency, GRNND adopts a reverse edge sampling strategy. For each vertex v with a neighbor set N_v of size k, reverse edges are inserted only for the top $\rho \cdot k$ neighbors, where $\rho \in (0, 1)$ is a configurable sampling ratio. This approach takes advantage of the randomness introduced by disordered propagation, ensuring sufficient structural perturbation without requiring additional randomization during edge insertion. Compared to exhaustive reverse insertion, this lightweight strategy reduces memory and computation overhead while using atomic writes only for the sampled subset to minimize contention and ensure correctness. At the same time, it effectively controls edge growth, preserves topological diversity, and supports convergence to high-quality graph structures at lower computational cost.

4 EXPERIMENTS

4.1 Experimental Setup

To comprehensively evaluate the performance of GRNND, we compare it against several state-of-the-art GPU-based ANNS algorithms as well as strong CPU baselines. Our primary focus is on index construction time, measured under comparable or equivalent search quality. We include the following representative algorithms for comparison.

- CAGRA[27]: A refinement-based GPU method that follows a build-then-prune paradigm.
- GANNS[37]: A GPU-optimized direct construction algorithm with enhancements inspired by NSW.
- GGNN[9]: A hierarchical GPU-based method designed for efficient graph generation.
- RNN[26]: The fastest known CPU implementation of RNN-Descent with high construction quality.
- HNSW[24]: A widely used CPU-based multi-layer graph structure optimized for search accuracy.
- GRNND: Our proposed GPU-parallel algorithm of RNN-Descent.

To ensure fair comparisons, we use a unified evaluation metric for index construction time. For flat graphs (non hierarchical), we first construct and save the index, then use the same search algorithm to evaluate Recall@10 and construction time under equivalent parameters. For hierarchical methods, we use their native search routines and match the neighbor pool sizes to maintain consistency. In addition to the core comparisons, we conducted ablation studies to isolate the impact of individual GRNND components and analyze how different hyperparameters affect both index construction time and search performance. All experiments were carried out in two hardware configurations: an NVIDIA RTX 4090 with an Intel Core i9-14900KF CPU and an NVIDIA RTX 6000 Ada with an AMD

Ryzen Threadripper PRO 7965WX CPU. The inclusion of both a consumer GPU and a professional GPU ensures the robustness of the results across different hardware environments.

4.2 Comparison with Other Methods

Figure 5 compares index construction time at matched recall across all methods on RTX 4090 and RTX 6000 Ada, respectively. For fairness, we fix the search algorithm and search parameter. The parameter corresponds to the maximum size of the candidate list maintained during graph traversal, while each method tunes only its construction configuration to reach a comparable Recall@10. GRNND consistently outperforms state-of-the-art GPU-based ANNS algorithms on both platforms, achieving comparable or better search quality with significantly lower construction time. On RTX 4090, GRNND achieves 2.6 to 3.9× speedup over GANNS, 3.1 to 5.0× over CAGRA, 21.5 to 48.3× over GGNN, 27.1 to 38.7× over CPU-based RNN and 31.9 to 49.8× over HNSW. On RTX 6000 Ada, GRNND achieves 2.4 to 4.1× speedup over GANNS, 4.3 to 5.7× over CAGRA, 30.6 to 51.7× over GGNN, 17.8 to 25.1× over CPU-based RNN and 22.7 to 26.2× over HNSW. The results demonstrate consistent advantages on both consumer- and professional-grade GPUs, thereby validating robustness across heterogeneous hardware environments.

Notably, GRNND demonstrates strong robustness to increasing dimensionality. Its construction time scales proportionally with vector dimension, maintaining high throughput even on high-dimensional datasets. This is primarily enabled by GRNND's warp-level cooperative computation, which parallelizes both distance calculations and neighbor updates with minimal divergence and memory contention. In the GIST1M dataset (960 dimensions), GRNND achieves its largest performance margin, highlighting its scalability. In contrast, GGNN and CAGRA show degraded performance under high dimensionality. GGNN suffers from excessive construction time and lower search accuracy due to ineffective hierarchical graph construction. CAGRA frequently fails to complete due to memory exhaustion before pruning and refinement phases. GRNND's superior performance is attributed to two key design elements: its fixed-capacity double-buffered pool, which ensures consistent and conflict-free memory access, and its disordered neighbor propagation strategy, which enhances structural diversity and avoids the convergence failures caused by globally synchronized updates. Together, these techniques allow GRNND to build high-quality graphs efficiently, even under challenging high-dimensional conditions.

Figure 6 shows CPU query performance using a unified search algorithm. The comparison is conducted across graphs built by each method under comparable construction configurations. After construction, all graphs are evaluated with the same search algorithm, and QPS−recall curves are obtained by varying the search parameter that controls the candidate list size. GRNND achieves search quality comparable to that of CPU-based RNN-Descent, confirming that our GPU-parallel design preserves graph quality. Moreover, the graphs generated by GRNND achieve search performance slightly higher than HNSW and substantially better than GPU-based GGNN and CAGRA. Since GRNND achieves the shortest construction time among all methods, this highlights the superiority of our GPU-parallel algorithm. Here, GANNS is excluded from the comparison
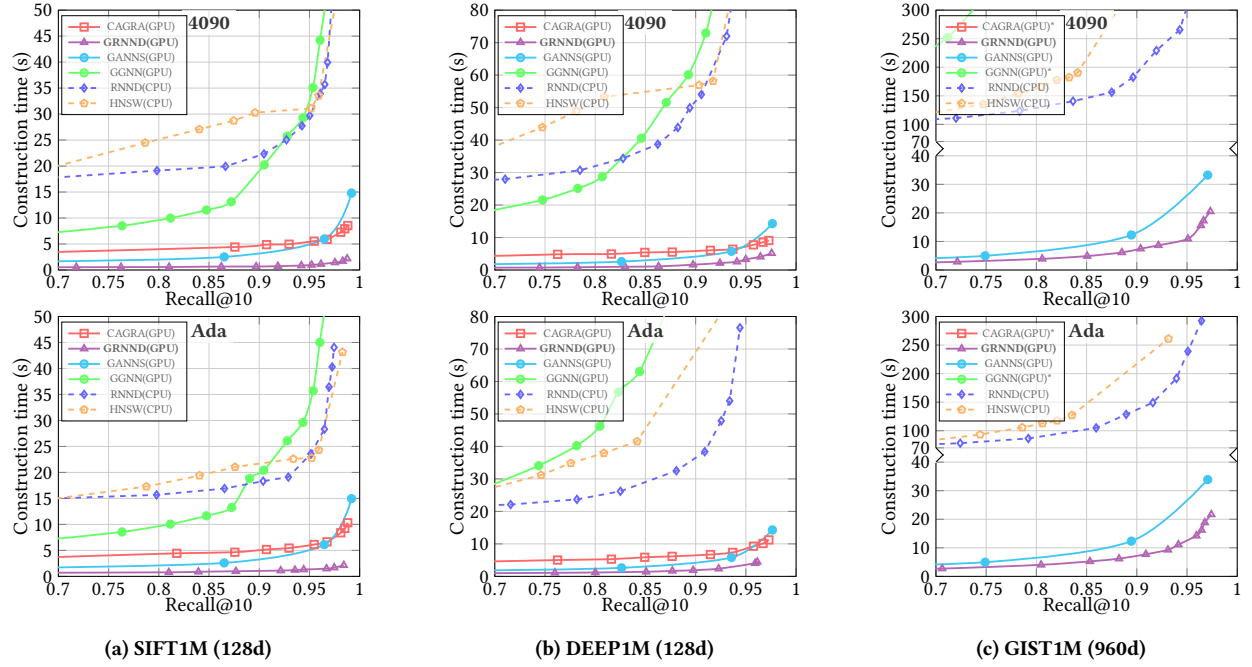
Figure 5: Evaluating construction time vs. recall: Fixed search settings with method-specific construction tuning for comparable Recall@10. *On GIST1M, CAGRA is unavailable due to high memory demand; GGNN is omitted due to excessive build time.*
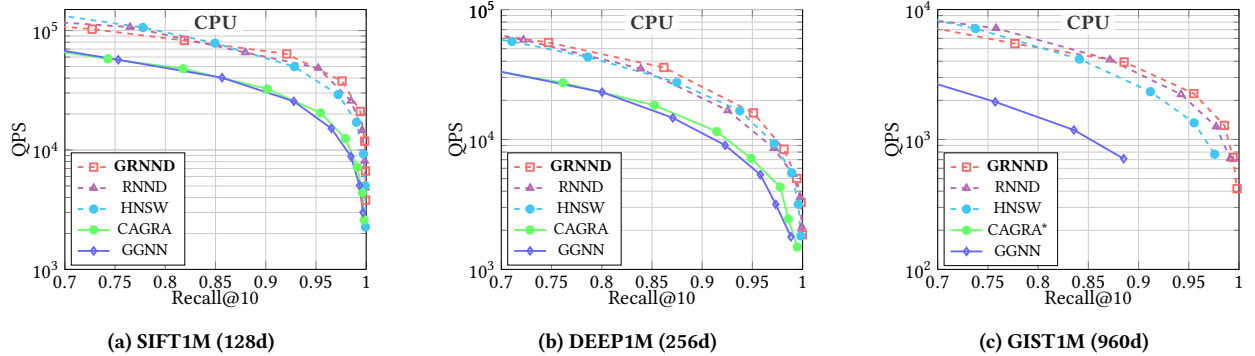

Figure 6: Evaluating QPS vs. recall: Fixed construction settings with method-specific search tuning to assess the performance of the constructed indices. *On GIST1M, CAGRA is unavailable due to high memory demand.*

since its index cannot be evaluated with a search algorithm independent of its native query implementation.

4.3 Ablation Study

Figures 7 and 8 evaluate the impact of various optimization strategies in GRNND on both RTX 4090 and RTX 6000 Ada. Both the fixed-capacity double-buffered structure and warp-level cooperative updates are always enabled as part of the baseline design.

Figure 7 compares the disordered execution strategy with ascending and descending sorting orders on the SIFT1M, DEEP1M, and GIST1M datasets. We include descending sorting to provide a comprehensive understanding of how the update order influences structural diversity and search accuracy. The observed trends are

consistent across both GPUs. Notably, the RTX 6000 Ada exhibits slightly longer construction time than the RTX 4090 under identical configurations. This is primarily due to differences in clock frequency and power configuration, as the professional-grade Ada architecture is tuned for sustained stability and large memory capacity rather than maximizing raw throughput, in contrast to the consumer-oriented RTX 4090.

Ascending sorting, which prioritizes nearest neighbors, tends to lead to synchronous convergence traps during parallel execution. When all vertices update their neighbors simultaneously, early convergence restricts topological diversity, which is particularly problematic in parallel GPU environments. On the other hand, descending sorting emphasizes distant neighbors, promoting better

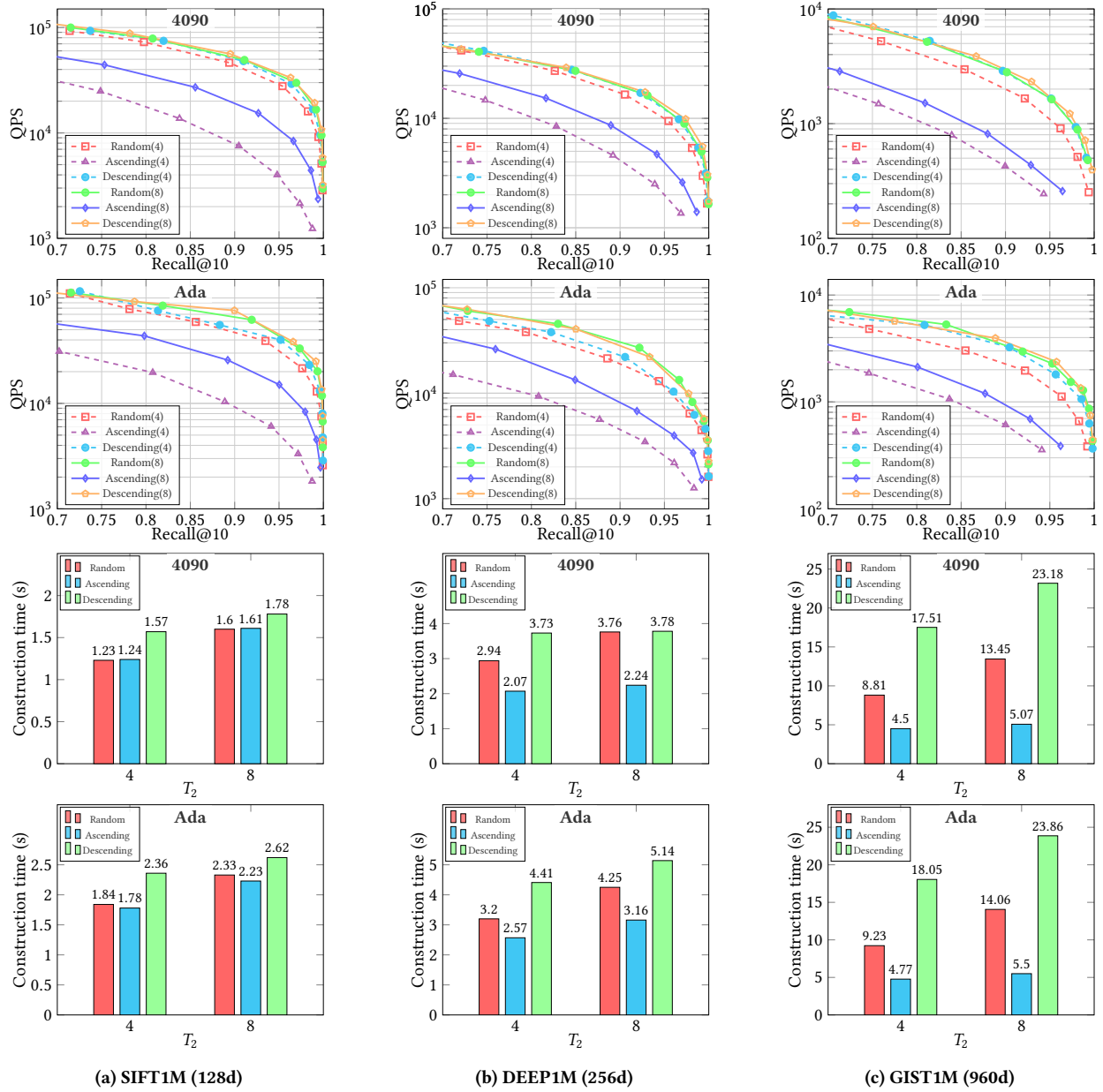(a) SIFT1M (128d) (b) DEEP1M (256d) (c) GIST1M (960d)

Figure 7: Performance under different candidate update strategies on GRNND across datasets: ascending may cause convergence traps, descending improves exploration but is costly, while random provides a balanced trade-off.

global exploration. However, this increases computational overhead, especially on high-dimensional datasets like GIST1M, as it requires excessive exploratory updates to maintain diversity. In contrast, disordered execution strikes a more balanced approach. By randomly selecting neighbor pairs for evaluation based on the RNG condition, disordered execution maintains structural diversity without incurring the overhead seen in descending sorting. While slightly slower than ascending sorting, disordered execution is much faster than descending sorting and achieves superior search accuracy. Thus, disordered execution avoids the convergence trap inherent in

ascending sorting and mitigates the overhead of descending sorting. This makes it an effective strategy for high-dimensional, large-scale graph construction.

Figure 8 illustrates the effect of varying the back-edge sampling ratio on the performance of GRNND across datasets. The overall trend of the RTX 4090 and RTX 6000 Ada is consistent, highlighting the robustness of the design. A low sampling ratio produces faster index construction, but reduces connectivity and structural diversity. This degradation is particularly pronounced on high-dimensional datasets such as GIST1M, where sparse neighborhoods
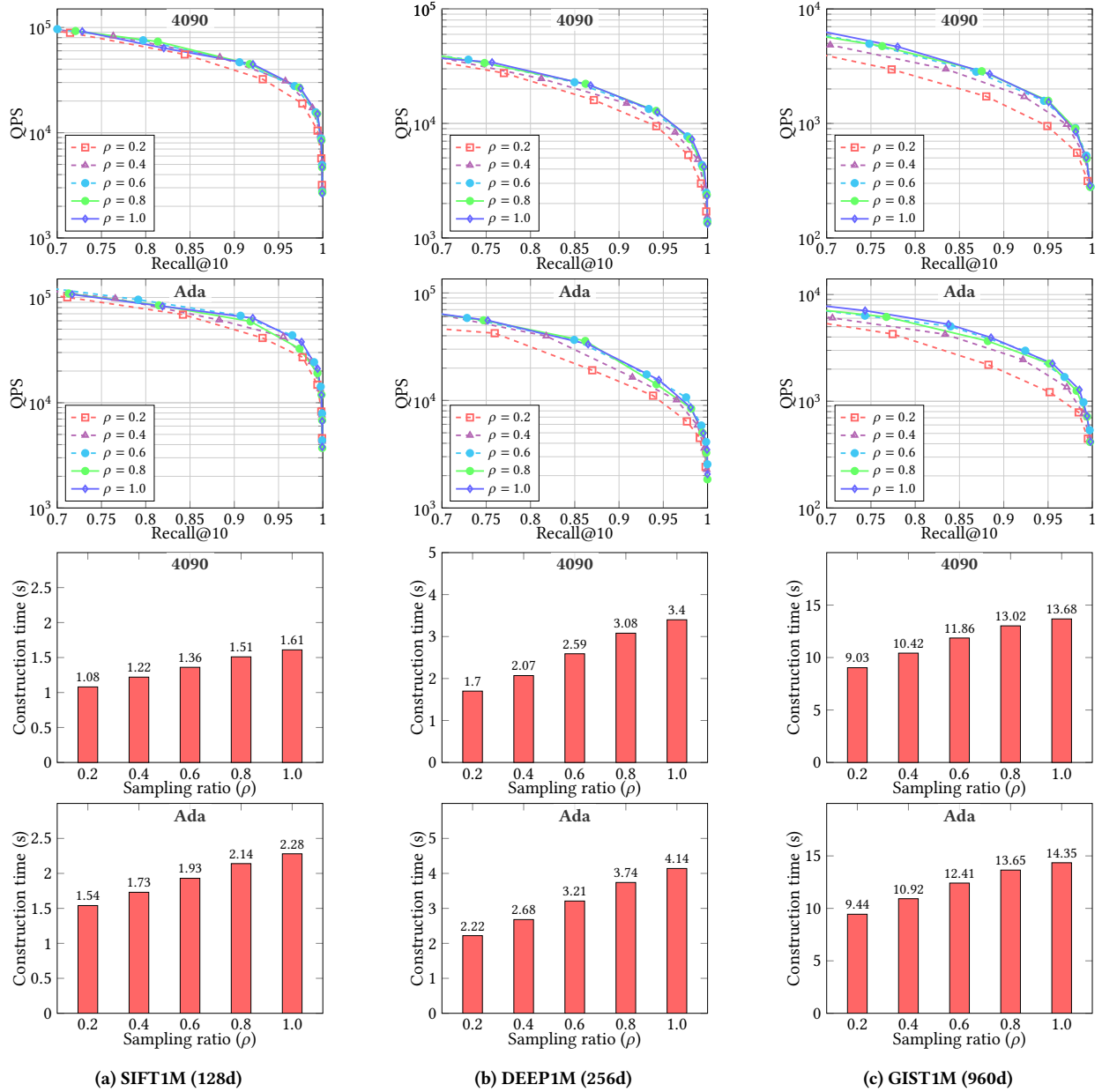
Figure 8: Performance under different back-edge Sampling ratio (ρ)s (reverse edges added) on GRNND across datasets: low ratios speed up but reduce accuracy, high ratios improve quality but slow down, while around 0.6 offers the best trade-off.

amplify the loss of reverse edges. Increasing the sampling ratio improves graph quality and search accuracy by incorporating more reverse connections, yet the gain diminishes once sufficient connectivity has been established. Beyond this point, further increases in the ratio no longer yield meaningful accuracy improvements but monotonically prolong construction time. This overhead arises because additional reverse neighbors enlarge the candidate pool and incur higher refinement costs during each iteration. Overall, the results demonstrate that a moderate sampling ratio (around 0.6) achieves

the best balance between efficiency and quality. It preserves sufficient structural diversity to sustain high recall while avoiding the excessive refinement overhead associated with higher ratios. Thus, careful tuning of the sampling ratio is essential for constructing high-quality graphs efficiently, especially in high-dimensional settings.
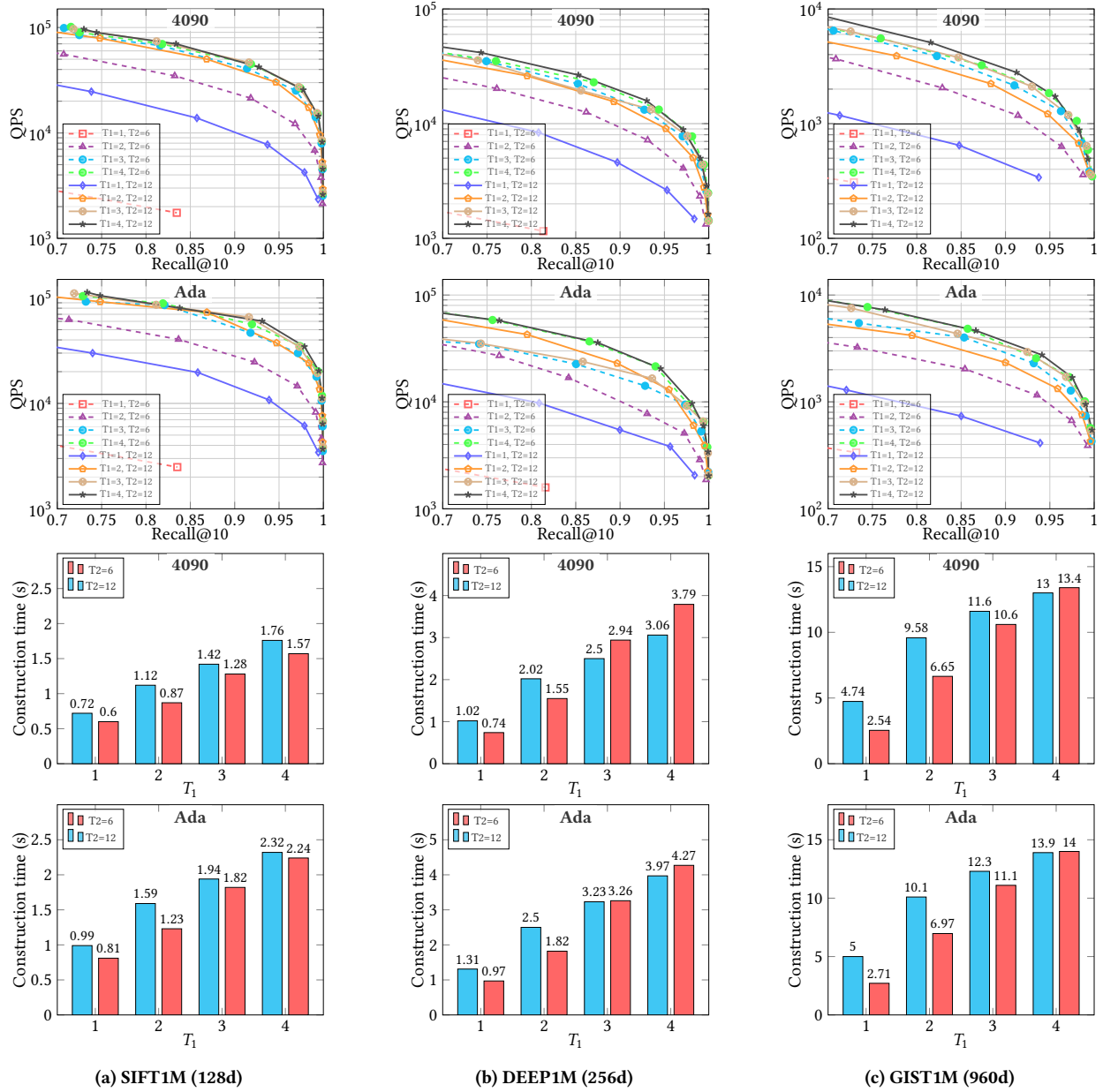
Figure 9: Performance under varying outer ($T1$) and inner ($T2$) iterations on GRNND across datasets: larger $T2$ improves accuracy but reduces efficiency, while higher $T1$ benefits mainly high-dimensional data at the cost of longer construction time.

4.4 Parameter Sensitivity

Figure 9 examines the influence of the outer iteration count (T_1) and the inner iteration count (T_2) on graph construction across the three benchmark datasets. The observed tendencies are consistent for both RTX 4090 and RTX 6000 Ada. The effect of T_2 exhibits a strong dependence on the dimensionality of the data. Increasing T_2 generally improves graph refinement and increases search accuracy, but its impact on construction time diverges between datasets. In SIFT1M, where the points are densely distributed, neighborhood

structures converge quickly in a few refinement steps. Additional T_2 iterations only introduce redundant comparisons and insertions, leading to a nearly monotonic increase in construction time. In contrast, on higher-dimensional datasets such as DEEP1M and GIST1M, where the neighborhoods are sparser and the initial quality of the candidate is lower, moderate increases in T_2 accelerate the formation of high-quality candidate pools in early iterations. This reduces redundant neighbor updates in later outer loops, and in some cases even shortens the overall construction time.

The role of T_1 is comparatively uniform: more outer iterations inevitably prolong the construction time, since each iteration entails a full graph refinement. However, the benefits are dimension-dependent. For low-dimensional datasets (SIFT1M, DEEP1M), one or two outer iterations already yield a near-optimal graph, with further rounds providing only marginal accuracy gains at significant time cost. In contrast, on the high-dimensional GIST1M, increasing T_1 continues to improve graph quality and recall, as repeated refinement is necessary to escape local optima and overcome the extreme sparsity of high-dimensional space.

In summary, both GPUs exhibit the same performance–quality trade-off: shallow optimization cycles suffice for low-dimensional data, while high-dimensional datasets demand deeper iterations to achieve competitive accuracy. The joint tuning of T_1 and T_2 is therefore essential to balance efficiency and quality, and consistent cross-platform trends further validate the generality of the proposed design.

5 RELATED WORK

Early GPU efforts mainly focused on the search stage, such as SONG [38] and FAISS [15]. As datasets scaled, index construction emerged as the primary bottleneck, motivating fully GPU-based solutions.

GNND[32], by Wang et al., is a GPU adaptation of NN-Descent. It uses selective neighbor updates to reduce global memory traffic and optimized sampling and distance computation to achieve 100 to 250× speedup over single-threaded NN-Descent, outperforming GPU baselines like GGNN and FAISS by 2.5 to 5×.

CAGRA[27], by Ono et al., is a GPU-Native framework for both construction and querying. It constructs an initial K-NN graph and refines it through pruning. With warp-segmented execution, forgettable hash tables, and topology-aware pruning, it significantly reduces memory and maintenance costs—achieving 2–27× speedup over HNSW in graph building.

GANNS[37], by Yu et al., is a GPU-parallel graph construction and search framework optimized for NSW and NSG. It uses CUDA-based concurrent node expansion and local atomics with global consistency checks to manage connections. Experiments demonstrate that it outperforms SONG and earlier GPU-HNSW methods in both speed and accuracy.

GGNN[9], by Groh et al., partitions the datasets into subsets, constructs subgraphs, and merges them hierarchically. It uses thread-block granularity for task division and employs hierarchical scheduling and unified neighbor pools to reduce contention. It surpasses FAISS in build speed.

6 CONCLUSION

This paper presents GRNND, the first GPU-parallel algorithm of Relative NN-Descent for efficient approximate nearest neighbor (ANN) graph construction. GRNND preserves the core refinement principles of RNN-Descent, but systematically redesigns its execution flow, memory organization, and update strategy to match the massively parallel architecture of modern GPUs. The main contributions include a disordered neighbor propagation strategy that mitigates synchronous convergence traps, a warp-cooperative update

mechanism that ensures both efficiency and correctness under concurrency, and a fixed-capacity double-buffered pool that avoids the overhead of dynamic allocation. These innovations jointly enable GRNND to deliver high-quality graphs with substantially reduced construction time. Extensive experiments on multiple datasets and hardware platforms demonstrate that GRNND consistently outperforms both CPU- and GPU-based baselines, validating its robustness across dimensionalities and system configurations. Future work will focus on extending GRNND to broader application scenarios, such as billion-scale indexing, multi-GPU or distributed deployments, and integration into end-to-end retrieval and analytics pipelines. Another promising direction is further system-level optimization, including memory management and scheduling policies, to maximize throughput on emerging GPU architectures.

Acknowledgments

References

[1] Dmitry Baranchuk, Artem Babenko, and Yury Malkov. 2018. Revisiting the inverted indices for billion-scale approximate nearest neighbors. In *Proceedings of the European Conference on Computer Vision (ECCV)*. Springer, 202–216.

[2] Fabio Carrara, Lucia Vadicamo, Claudio Gennaro, and Giuseppe Amato. 2022. Approximate nearest neighbor search on standard search engines. In *International Conference on Similarity Search and Applications*. Springer International Publishing, 214–221.

[3] Qiong Chang, Xiang Li, Yun Li, and Jun Miyazaki. 2023. Multi-directional Sobel operator kernel on GPUs. *J. Parallel and Distrib. Comput.* 177 (2023), 160–170.

[4] Qiong Chang, Weimin Wang, and Jun Miyazaki. 2025. Accelerating Nearest Neighbor Search in 3D Point Cloud Registration on GPUs. *ACM Transactions on Architecture and Code Optimization* (2025).

[5] Wei Dong, Charikar Moses, and Kai Li. 2011. Efficient k-nearest neighbor graph construction for generic similarity measures. In *Proceedings of the 20th International Conference on World Wide Web*. 577–586.

[6] Cong Fu, Changxu Wang, and Deng Cai. 2021. High dimensional similarity search with satellite system graph: Efficiency, scalability, and unindexed query compatibility. *IEEE Transactions on Pattern Analysis and Machine Intelligence* 44, 8 (2021), 4139–4150.

[7] Cong Fu, Chao Xiang, Changxu Wang, and Deng Cai. 2017. Fast approximate nearest neighbor search with the navigating spreading-out graph. arXiv preprint arXiv:1707.00143.

[8] Trevor Gale, Matei Zaharia, Cliff Young, and Erich Elsen. 2020. Sparse gpu kernels for deep learning. In *SC20: International Conference for High Performance Computing, Networking, Storage and Analysis*. IEEE, 1–14.

[9] Fabian Groh, Lukas Ruppert, Patrick Wieschollek, and Hendrik PA Lensch. 2022. Ggnn: Graph-based gpu nearest neighbor search. *IEEE Transactions on Big Data* 9, 1 (2022), 267–279.

[10] Gaurav Gupta, Tharun Medini, Anshumali Shrivastava, and Alexander J. Smola. 2022. Bliss: A billion scale index using iterative re-partitioning. In *Proceedings of the 28th ACM SIGKDD Conference on Knowledge Discovery and Data Mining*. 486–495.

[11] Ben Harwood and Tom Drummond. 2016. Fanng: Fast approximate nearest neighbour graphs. In *Proceedings of the IEEE Conference on Computer Vision and Pattern Recognition*. 5713–5722.

[12] Jui-Ting Huang, Ashish Sharma, Shuying Sun, Li Xia, David Zhang, Philip Pronin, Janani Padmanabhan, Giuseppe Ottaviano, and Linjun Yang. 2020. Embedding-based retrieval in facebook search. In *Proceedings of the 26th ACM SIGKDD International Conference on Knowledge Discovery & Data Mining*. 2553–2561.

[13] Jerzy W Jaromczyk and Godfried T Toussaint. 2002. Relative neighborhood graphs and their relatives. *Proc. IEEE* 80, 9 (2002), 1502–1517.

[14] Sian Jin, Pascal Grosset, Christopher M. Biwer, Jesus Pulido, Jiannan Tian, Dingwen Tao, and James Ahrens. 2020. Understanding GPU-based lossy compression for extreme-scale cosmological simulations. In *2020 IEEE International Parallel and Distributed Processing Symposium (IPDPS)*. IEEE, 105–115.

[15] Jeff Johnson, Matthijs Douze, and Hervé Jégou. 2019. Billion-scale similarity search with GPUs. *IEEE Transactions on Big Data* 7, 3 (2019), 535–547.

[16] Conglong Li, Minjia Zhang, David G. Andersen, and Yuxiong He. 2020. Improving approximate nearest neighbor search through learned adaptive early termination. In *Proceedings of the 2020 ACM SIGMOD International Conference on Management of Data.* 2539–2554.

[17] Wen Li, Ying Zhang, Yifang Sun, Wei Wang, Mingjie Li, Wenjie Zhang, and Xuemin Lin. 2019. Approximate nearest neighbor search on high dimensional data—experiments, analyses, and improvement. *IEEE Transactions on Knowledge and Data Engineering* 32, 8 (2019), 1475–1488.

[18] Xiang Li, Qiong Chang, Yun Li, and Jun Miyazaki. 2025. 3D GNLM: Efficient 3D Non-Local Means Kernel with Nested Reuse Strategies for Embedded GPUs. *ACM Trans. Archit. Code Optim.* (2025).

[19] Xiang Li, Qiong Chang, Aolong Zha, Shijie Chang, Yun Li, and Jun Miyazaki. 2024. An Optimized GPU Implementation for GIST Descriptor. *ACM Transactions on Architecture and Code Optimization* 21, 4 (2024), 1–24.

[20] Junhan Liu, Zinuo Cai, Yumou Liu, Hao Li, Zongpu Zhang, Ruhui Ma, and Rajkumar Buyya. 2025. SMore: Enhancing GPU Utilization in Deep Learning Clusters by Serverless-based Co-location Scheduling. *IEEE Transactions on Parallel and Distributed Systems* (2025).

[21] Jun Liu, Zhenhua Zhu, Jingbo Hu, Hanbo Sun, Li Liu, Lingzhi Liu, Guohao Dai, Huazhong Yang, and Yu Wang. 2022. Optimizing graph-based approximate nearest neighbor search: Stronger and smarter. In *2022 23rd IEEE International Conference on Mobile Data Management (MDM).* IEEE, 179–184.

[22] Jingjia Luo, Mingxing Zhang, Kang Chen, Xia Liao, Yingdi Shan, Jinlei Jiang, and Yongwei Wu. 2025. Efficient Graph-Based Approximate Nearest Neighbor Search Achieving: Low Latency Without Throughput Loss. *arXiv preprint arXiv:2504.20461* (2025).

[23] Yury Malkov, Alexander Ponomarenko, Andrey Logvinov, and Vladimir Krylov. 2014. Approximate nearest neighbor algorithm based on navigable small world graphs. *Information Systems* 45 (2014), 61–68.

[24] Yu A. Malkov and Dmitry A. Yashunin. 2018. Efficient and robust approximate nearest neighbor search using hierarchical navigable small world graphs. *IEEE Transactions on Pattern Analysis and Machine Intelligence* 42, 4 (2018), 824–836.

[25] Bruno Meyer, Aurora Pozo, and Wagner M Nunan Zola. 2021. Warp-centric k-nearest neighbor graphs construction on GPU. In *50th International Conference on Parallel Processing Workshop.* 1–10.

[26] Naoki Ono and Yusuke Matsui. 2023. Relative nn-descent: A fast index construction for graph-based approximate nearest neighbor search. In *Proceedings of the 31st ACM International Conference on Multimedia.* 1659–1667.

[27] Hiroyuki Ootomo, Akira Naruse, Corey Nolet, Ray Wang, Tamas Feher, and Yong Wang. 2024. Cagra: Highly parallel graph construction and approximate nearest neighbor search for gpus. In *2024 IEEE 40th International Conference on Data Engineering (ICDE).* IEEE, 4236–4247.

[28] Jiancheng Ruan, Tingyang Chen, Renchi Yang, Xiangyu Ke, and Yunjun Gao. 2025. Empowering Graph-based Approximate Nearest Neighbor Search with Adaptive Awareness Capabilities. *arXiv preprint arXiv:2506.15986* (2025).

[29] Zhengkai Tu, Wei Yang, Zihang Fu, Yuqing Xie, Luchen Tan, Kun Xiong, Ming Li, and Jimmy Lin. 2020. Approximate nearest neighbor search and lightweight dense vector reranking in multi-stage retrieval architectures. In *Proceedings of the 2020 ACM SIGIR on International Conference on Theory of Information Retrieval.* 97–100.

[30] Karthik V., Saim Khan, Somesh Singh, Harsha Vardhan Simhadri, and Jyothi Vedurada. 2025. BANG: Billion-Scale Approximate Nearest Neighbour Search using a Single GPU. *IEEE Transactions on Big Data* (2025), 1–16.

[31] Thomas Vecchiato, Claudio Lucchese, Franco Maria Nardini, and Sebastian Bruch. 2024. A learning-to-rank formulation of clustering-based approximate nearest neighbor search. In *Proceedings of the 47th International ACM SIGIR Conference on Research and Development in Information Retrieval.* 2261–2265.

[32] Hui Wang, Wan-Lei Zhao, Xiangxiang Zeng, and Jianye Yang. 2021. Fast k-nn graph construction by gpu based nn-descent. In *Proceedings of the 30th ACM International Conference on Information & Knowledge Management.* 1929–1938.

[33] Mengzhao Wang, Haotian Wu, Xiangyu Ke, Yunjun Gao, Yifan Zhu, and Wenchao Zhou. 2025. Accelerating Graph Indexing for ANNS on Modern CPUs. *Proceedings of the ACM on Management of Data* 3, 3 (2025), 1–29.

[34] Mengzhao Wang, Xiaoliang Xu, Qiang Yue, and Yuxiang Wang. 2021. A comprehensive survey and experimental comparison of graph-based approximate nearest neighbor search. arXiv preprint arXiv:2101.12631.

[35] Patrick Wieschollek, Oliver Wang, Alexander Sorkine-Hornung, and Hendrik Lensch. 2016. Efficient large-scale approximate nearest neighbor search on the GPU. In *Proceedings of the IEEE Conference on Computer Vision and Pattern Recognition.* 2027–2035.

[36] Lee Xiong, Chenyan Xiong, Ye Li, Kwok-Fung Tang, Jialin Liu, Paul Bennett, Junaid Ahmed, and Arnold Overwijk. 2020. Approximate nearest neighbor negative contrastive learning for dense text retrieval. arXiv preprint arXiv:2007.00808.

[37] Yuanhang Yu, Dong Wen, Ying Zhang, Lu Qin, Wenjie Zhang, and Xuemin Lin. 2022. GPU-accelerated proximity graph approximate nearest Neighbor search and construction. In *2022 IEEE 38th International Conference on Data Engineering (ICDE).* IEEE, 552–564.

[38] Weijie Zhao, Shulong Tan, and Ping Li. 2020. Song: Approximate nearest neighbor search on gpu. In *2020 IEEE 36th International Conference on Data Engineering (ICDE).* IEEE, 1033–1044.